Weak-localization approach to a 2D electron gas with a spectral node

Klaus G. Ziegler, Andreas Sinner

Angaben zur Veröffentlichung / Publication details:

Ziegler, Klaus G., and Andreas Sinner. 2015. "Weak-localization approach to a 2D electron gas with a spectral node." *Physica E: Low-dimensional Systems and Nanostructures* 71: 14–20. https://doi.org/10.1016/j.physe.2015.03.017.

Weak-localization approach to a 2D electron gas with a spectral node

K. Ziegler *, A. Sinner

Institut für Physik, Universität Augsburg, D-86135 Augsburg, Germany

1. Introduction

The weak-localization approach (WLA) has been a very popular tool to estimate whether electronic states in a weakly disordered system tend to localize or to delocalize on large scales. A central result of the WLA is that on large scales there might be diffusion due to one or more undamped modes. This has been studied in great detail for conventional metals [1–3] and more recently for graphene [4,5] and for the surface of topological insulators [6,7], using a one-band projection for the two-band system. The existence of a diffusive mode, which is a necessary (but not a sufficient) condition for metallic behavior, has been debated for the one-band projected graphene model. It was found that either a single diffusive channel exists [4,6,7] or no diffusion [5] in the presence of generic disorder.

The WLA is usually based on an analysis of the current–current Kubo conductivity [4]

$$\sigma_{\mu\mu} \sim \frac{1}{\pi\hbar}\langle \mathrm{Tr}\left(j_\mu G j_\mu G^\dagger\right)\rangle. \tag{1}$$

The main reason for this choice is that the current–current correlation function $\langle \mathrm{Tr}(j_\mu G j_\mu G^\dagger)\rangle$ is related to the action of the corresponding nonlinear sigma model $(1/2t)\int \mathrm{Tr}(\partial_\mu Q \partial_\mu Q)$ of the matrix field Q [2], since the current operator j_μ of a conventional one-band model is proportional to the momentum operator $-i\partial_\mu$. Therefore, the renormalization of the parameter t corresponds to the renormalization of the current–current correlation function. This relation, however, breaks down for Dirac fermions, where j_μ is proportional to the Pauli matrix σ_μ. For this reason it is not obvious that the renormalization of the nonlinear sigma model is linked to the renormalization of the current–current correlation function.

An alternative to the WLA is the weak-scattering approach (WSA), where transport properties are studied within the expansion in powers of η/E_b (η is the scattering rate and E_b is the bandwidth) [8]. A non-Abelian chiral symmetry was identified, which describes diffusion in two-band systems due to spontaneous symmetry breaking [9]. This is also the origin of a undamped fermion mode found for 2D Dirac fermions with a random gap in Ref. [10]. In the WSA disorder fluctuations of the two-band model are approximated by Gaussian fluctuations around a saddle-point of the original model, expressed in terms of a functional integral [8]. The saddle point is equivalent to the self-consistent Born approximation (SCBA) of the one-particle Green's function, while the Gaussian fluctuations are related to the WLA. The latter consists of one-particle and two-particle diagrams which are partially summed up in terms of geometric series (cf. Section 3). Within the WSA it is also possible to analyze the fluctuations with respect to the non-Abelian chiral symmetry. The projection onto these fluctuations generates a nonlinear field which allows us to go beyond the Gaussian approximation within the expansion in powers of η/E_b. This idea is analogous to the nonlinear sigma model, derived originally for one-band Hamiltonians by Schäfer and Wegner [11]. The difference between the one-band and the two-band Hamiltonians is that the former can be formulated either in a symmetric replica space or in a supersymmetric fermion–boson space [12], whereas the latter can also be expressed in terms of a non-symmetric fermion–boson theory [10]. Therefore, in the derivation of a nonlinear sigma model it is crucial to take the two-band structure into account. A projection onto a single

* Corresponding author. Fax: +49 821 598 3262.
E-mail address: klaus.ziegler@physik.uni-augsburg.de (K. Ziegler).

band could destroy the relevant symmetries of the system. In more physical terms, the two-band structure is essential for supporting diffusion in a two-dimensional system, since it allows for Klein tunneling. The latter enables a particle in a potential barrier to transmute to a hole, for which the potential barrier is not an obstacle. Our aim is to establish a direct connection between the WLA and the Gaussian fluctuations around the saddle point for 2D Dirac fermions with a random gap, and to provide a general discussion about the existence of diffusive modes due to ladder and maximally crossed contributions in two-band systems. Finally, these results will be employed to calculate the conductivity corrections, and the resulting conductivities will be compared with experimental measurements in graphene. The results can also be applied to other 2D two-band systems such as the surface of topological insulators [13].

1.1. Motivation for the subsequent calculation

Since the subsequent calculations of the WLA are lengthy, we give a brief summary and explain our motivation for this work.

The central idea of the WLA is a perturbation expansion of the average Green's functions in terms of disorder, where certain types of diagrams are summed up to infinite order. In particular, the average two-particle Green's function can be approximated by summing up ladder diagrams and maximally crossed diagrams (cf. Fig. 1). These sums are obtained from the iteration of a Bethe–Salpeter equation. All this is well known from numerous studies [1–3,14]. However, only recently the case of a two-band Hamiltonian has been considered [4–7]. In comparison with the one-band Hamiltonian this requires an extension of previous calculations, since Green's functions have poles in the upper as well as in the lower band. The above-mentioned calculations have projected out the poles in one band, but keeping the spinor structure of Green's function. Although it is plausible that this should be a valid approximation if the Fermi energy is in the other band far away from the omitted pole, it needs to be checked how the approximation affects the symmetries of the model and the related diffusive modes. For this purpose we employ in this work the WLA for the full two-band (spinor) Green's function and compare the results with the one-band projected poles in Section 6. It turns out that the diffusive modes are not destroyed by the projection, although the diffusion coefficients are different. Another motivation for this work was that previous calculations of the conductivity within the WLA were based on the current–current Kubo formula. The quantum fluctuations gave a logarithmically divergent correction to the classical Drude (or Boltzmann) result, which must be cut-off by a phenomenological inelastic scattering length. This problem can be circumvented by using the density–density representation of the Kubo formula [15], for which the conductivity, as a function of charge density, has a V-shape form (cf. Eq. (43) and Fig. 2), in agreement with the experimental observation. This result was previously also found within the WSA [9].

The agreement of the WLA and the WSA results in terms of the density–density Kubo formula motivated us to compare the two approaches in more detail. It is possible to identify the ladder (maximally crossed) diagrams with fermionic (bosonic) fluctuations of the effective fermion–boson representation of the WSA.

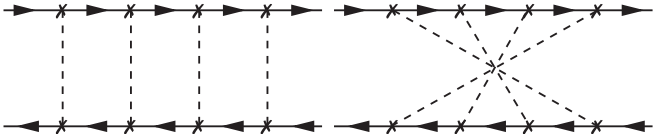

Fig. 1. Diagrammatic representation of the fourth order terms for the ladder contribution of $(\mathbf{1} - t)^{-1}$ and maximally crossed contributions of $(\mathbf{1} - \tau)^{-1}$, respectively.

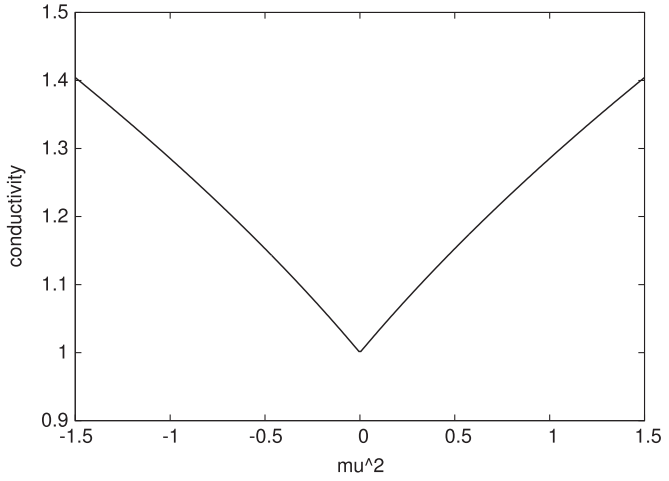

Fig. 2. DC conductivity as a function of $\zeta^2 = \mu^2/\eta^2$ from the expression in Eq. (43).

Thus the difference of the two types of diagrams reflects the spontaneous symmetry breaking in the WSA.

Measurements of the field- and temperature dependent magnetoresistance, for instance, at graphene samples provide an indirect test for the quality of the WLA. The corresponding calculation uses as a starting point the diffusion propagator with minimal coupling to the vector potential of a homogeneous magnetic field [3]. This leads to a rather universal expression for the magnetoresistance in terms of logarithmic and digamma functions whose parameters are the magnetic field, scaled with various scattering times. We expect a similar result for the magnetoresistance from our unprojected propagators. On the other hand, the interplay of different values of scattering times affects the question whether there is weak localization or weak antilocalization [16,17]. In particular, the final result depends crucially on the inelastic scattering time, which can only be determined empirically as functions of temperature. Thus, the magnetoresistance of graphene-like materials is not a very robust quantity to distinguish between localization and antilocalization within the WLA, and it is better to consider the conductivity without magnetic field instead.

The paper is organized as follows. In Section 2 we introduce a general description for the two-band Hamiltonian and various types of random scattering. The main ideas of the WLA are discussed in Section 3, which includes the self-consistent Born approximation for the average one-particles Green's function, the ladder and the maximally crossed contribution of the average two-particle Green's function. In Section 4 we study the long-range behavior of the average two-particle Green's function for a one-band Hamiltonian (Section 4.1) and for the two-band Hamiltonian (Section 4.2). These results are used to calculate the conductivity (Section 5). And finally, in Section 6 we discuss the connection of the WLA with the WSA, the robustness of the diffusion pole structure with respect to a one-band projection of the two-band Hamiltonian and the symmetry properties of the inter-node scattering.

2. Model: Hamiltonians, Green's functions and symmetries

Quasiparticles in a system with two bands are described by a spinor wavefunction. The corresponding Hamiltonian can be expanded in terms of Pauli matrices $\sigma_{0,1,2,3}$. Here we will consider either a gapless Hamiltonian

$$H_0 = h_1\sigma_1 + h_2\sigma_2 \tag{2}$$

or a gapped Hamiltonian

$$H_m = h_1\sigma_1 + h_2\sigma_2 + m\sigma_3. \tag{3}$$

The gapless Hamiltonian changes its sign under a chiral transformation

$$\sigma_3 H_0 \sigma_3 = -H_0, \tag{4}$$

which implies the continuous Abelian chiral symmetry

$$e^{\alpha\sigma_3} H_0 e^{\alpha\sigma_3} = H_0.$$

The situation is more subtle for H_m because its transformation properties depend on the properties of $h_{1,2}$. We distinguish here two cases, namely $h_j^T = -h_j$ (Dirac fermions, ^{T} is the transposition, acting on real space), where

$$\sigma_1 H_m^T \sigma_1 = -H_m \tag{5}$$

and $h_j^T = h_j$ (e.g., bilayer graphene), where

$$\sigma_2 H_m^T \sigma_2 = -H_m. \tag{6}$$

The transformation properties of the Hamiltonians imply a relation between the wavefunctions in the upper and in the lower band. In particular, Eq. (4) implies that $\Psi_{-E} = \sigma_3\Psi_E$, Eq. (5) implies that $\Psi_{-E} = \sigma_1\Psi_E^*$ and Eq. (6) that $\Psi_{-E} = \sigma_2\Psi_E^*$.

Disorder is included by an additional random term $\mathrm{diag}(v_1, v_2)$ in the Hamiltonians H_0 and H_m. In the following we will consider the case of $v_1 = v_2$ (scalar potential), $v_1 = -v_2$ (random gap) and independent random diagonal elements v_1, v_2, assuming that the matrix elements $v_{1,2}$ have mean zero and variance g.

3. Dyson and Bethe–Salpeter equation

3.1. Dyson equation

Starting point of the WLA is that Green's function $G_0(\mu - i\delta) = (H_0 - \mu + i\delta)^{-1}$ of the Hamiltonian H_0 is perturbed by V and creates Green's function $G = (G_0^{-1} + V)^{-1}$. The latter relation is equivalent to the matrix identity $G = G_0 - G_0VG$ which connects the unperturbed Green's function G_0 with the perturbed Green's function G. This equation can be iterated to give a geometric series

$$\begin{aligned} G &= G_0 - G_0VG \\ &= G_0 - G_0VG_0 + G_0VG_0VG \\ &= \cdots \\ &= G_0 \sum_{l\geq 0} (-VG_0)^l. \end{aligned} \tag{7}$$

Now we assume that V is a random quantity with mean $\langle V\rangle = 0$ such that the averaged Dyson equation becomes

$$\langle G\rangle = G_0 + G_0\langle VG_0VG\rangle. \tag{8}$$

When we assume that the correlation between Green's function and V is weak, the factorization of the average $\langle VG_0VG\rangle \approx \langle VG_0V\rangle\langle G\rangle$ is possible, which creates a linear equation for $\langle G\rangle$:

$$\langle G\rangle \approx G_0 + G_0\langle VG_0V\rangle\langle G\rangle, \tag{9}$$

whose solution reads $\langle G\rangle \approx (G_0^{-1} - \langle VG_0V\rangle)^{-1}$. This result is known as the Born approximation with the self-energy $\langle VG_0V\rangle$. The self-consistent Born approximation (SCBA) is provided by the replacement

$$\langle V_i G_{0,ij} V_j\rangle \to \langle V_i V_j\rangle\langle G_{ij}\rangle =: \Sigma_{ij} \tag{10}$$

on the right-hand side of Eq. (9):

$$\langle G\rangle \approx \bar{G} = (G_0^{-1} - \Sigma)^{-1}. \tag{11}$$

3.2. Bethe–Salpeter equation

The two-particle Green's function G^+G^-, created from the two one-particle Green's functions $G^\pm$ (e.g., the advanced and the retarded Green's function), reads with the help of the corresponding Dyson equations (7) (using the summation convention in this section)

$$\begin{aligned} &\langle G^+_{ij}G^-_{kl}\rangle = \langle T^{-1}_{ik,mn}\rangle G^+_{0,mj}G^-_{0,nl} \quad \text{with} \\ &T_{ik,mn} = \delta_{im}\,\delta_{kn} - G^+_{0,im'}V_{m'm}\,G^-_{0,kn'}V_{n'n}. \end{aligned} \tag{12}$$

On the left-hand side is the two-particle Green's function, while the right-hand side depends only on products of G_0. This equation is known as the Bethe–Salpeter equation. Now we can perform the average with respect to the random scatterers $V_{jj'}$, assuming that this is a Gaussian variable with zero mean. Here it is convenient to define $\gamma^\pm_{im} = G^\pm_{0,im'}V_{m'm}$ such that

$$T_{ik,mn} = \delta_{im}\,\delta_{kn} - \gamma^+_{im}\gamma^-_{kn}. \tag{13}$$

The expansion of T^{-1} leads to a geometric series in $\gamma^+_{m_1m_2}\gamma^-_{n_1n_2}$. Averaging this series with respect to a Gaussian distribution can be achieved by what is known as Wick's theorem: the average of the product of random variable $\langle V_m V_n \cdots\rangle$ is expressed as a sum over all possible products of pairs $\langle V_m V_n\rangle\cdots$. This series includes a ladder contribution and a maximally crossed contribution [14] (cf. Fig. 1) as special cases. We also include the contribution from the iterated Dyson equation of Section 3.1 in terms of the SCBA and obtain eventually

$$\langle G^+_{ij}G^-_{kl}\rangle \approx [\langle T^{-1}_{ik,mn}\rangle_L + \langle T^{-1}_{ik,mn}\rangle_M - \delta_{im}\,\delta_{kn} - t_{ik,mn}]\bar{G}^+_{mj}\bar{G}^-_{nl}, \tag{14}$$

where the last two terms on the right-hand side are introduced to avoid overcounting in the geometric series.

Beginning with the ladder contribution, we obtain

$$\begin{aligned} \langle T^{-1}_{ik,mn}\rangle_L &= (\mathbf{1} - t)^{-1}_{ik,mn} \quad \text{with } t_{m_1n_1,m_2n_2} \\ &= \langle \bar{G}^+_{m_1m_1}V_{m_1m_2}\bar{G}^-_{n_1n_1}V_{n_1n_2}\rangle. \end{aligned} \tag{15}$$

Then the maximally crossed contribution is created by re-arranging the order of factors in the geometric series which after averaging results in

$$\begin{aligned} \langle T^{-1}_{ik,mn}\rangle_M &= (\mathbf{1} - \tau)^{-1}_{in,mk} \quad \text{with } \tau_{m_1m_1',m_2m_2'} \\ &= \langle \bar{G}^+_{m_1n_1}V_{n_1m_2}\bar{G}^-_{m_2n_1}V_{n_1m_1'}\rangle. \end{aligned} \tag{16}$$

Thus, switching from the ladder contribution to the maximally crossed contribution is achieved simply through changing γ^- by the transposition $\gamma^-_{m_1'm_2} \to \gamma^-_{m_2m_1'}$.

In the following we will discuss the two-particle Green's functions of (14)–(16) and the SCBA for the two-band Hamiltonians of Section 2 with an additional random term $\mathrm{diag}(v_1, v_2)$, which is either a random scalar potential, a random gap or independent random diagonal elements. For simplicity it is assumed that the random terms are spatially uncorrelated.

4. Special cases of the two-particle Green's function

The general expressions in (15) and in (16) shall now be applied to specific cases. For a diagonal random matrix $V_{mm'} = V_m\,\delta_{m,m'}$ we obtain

$$\begin{aligned} t_{m_1n_1,m_2n_2} &= \bar{G}^+_{m_1m_2}\bar{G}^-_{n_1n_2}\langle V_{m_2}V_{n_2}\rangle, \\ \tau_{m_1n_1,m_2n_2} &= \bar{G}^+_{m_1m_2}\bar{G}^-_{n_2n_1}\langle V_{m_2}V_{n_1}\rangle. \end{aligned} \tag{17}$$

4.1. Scalar Green's function

Before we start to discuss the two-band Hamiltonians, the simpler one-band Hamiltonian with Fourier components $h(k)$ is used to explain briefly the main ideas of the WLA. For this case we consider the following coordinates in real space: $i = k = r$, $m = n = r'$. Then the ladder and the maximally crossed contributions read for uncorrelated disorder $\langle V_r V_{r'}\rangle = g\delta_{r,r'}$

$$t_{r1r2,r3r4} = g\bar{G}^{+}_{r1r3}\bar{G}^{-}_{r2r3}\delta_{r3,r4}, \quad \tau_{r1r2,r3r4} = g\bar{G}^{+}_{r1r3}\bar{G}^{-}_{r4r3}\delta_{r2,r3}, \tag{18}$$

and in the geometric series $\sum_{l\geq 0} t^{l}_{rr,r'r'}$ ($\sum_{l\geq 0} \tau^{l}_{rr',r'r}$) only

$$t_{r2r3} := t_{r2r2,r3r3} = g\bar{G}^{+}_{r2r3}\bar{G}^{-}_{r2r3}, \quad \tau_{r2r3} := \tau_{r2r3,r3r2} = g\bar{G}^{+}_{r2r3}\bar{G}^{-}_{r2r3} \tag{19}$$

contributes. Thus Eq. (14) reads

$$\langle G^{+}_{rr'}G^{-}_{rr'}\rangle \approx \sum_{r''}[(\mathbf{1}-t)^{-1}_{rr''} + (\mathbf{1}-\tau)^{-1}_{rr''} - \delta_{rr''} - t_{rr''}]\bar{G}^{+}_{r''r'}\bar{G}^{-}_{r''r'}. \tag{20}$$

Moreover, with (19) the extra factor $\bar{G}^{+}_{r''r'}\bar{G}^{-}_{r''r'}$ can be replaced by t/g or τ/g through the identity

$$\bar{G}^{+}_{r''r'}\bar{G}^{-}_{r''r'} = \frac{1}{g}t_{r''r'} = \frac{1}{g}\tau_{r''r'}. \tag{21}$$

This provides eventually

$$\langle G^{+}_{rr'}G^{-}_{rr'}\rangle \approx \frac{1}{g}(\mathbf{1}-t)^{-1}_{rr'} + \frac{1}{g}(\mathbf{1}-\tau)^{-1}_{rr'} - \frac{1}{g}(t^{2}_{rr'} + t_{rr'} + 2\delta_{rr'}). \tag{22}$$

Green's function is symmetric in the absence of a magnetic field, such that the Fourier components of the Hamiltonian $h(k)$ satisfy the relation $h(-k) = h(k)$. Then there is no difference between ladder and maximally crossed contributions. We consider $q \sim 0$ for the long-range behavior and obtain from the expansion in powers of the momentum q

$$t_q \sim g\sum_r \bar{G}^{+}_{r0}\bar{G}^{-}_{0r} - q^2\frac{g}{2}\sum_r r^2_{\mu}\bar{G}^{+}_{r0}\bar{G}^{-}_{0r} \tag{23}$$

and use the SCBA with the self-energy $\Sigma^{\pm}$: $\bar{G}^{+} = G_0(z)$, $\bar{G}^{-} = G_0(z)^{*}$ with $z = \mu - i\delta + \Sigma^{+}$. This gives $t_0 \sim 1 - 2i\delta/(z - z^{*})$, such that $K_q = 1/(1-t_q)$ becomes the diffusion propagator for $q \sim 0$

$$K_q = \frac{1}{1-t_q} \sim \frac{1}{2i\delta/(z-z^{*}) + q^2(g/2)\sum_r r^2_{\mu}\bar{G}^{+}_{r0}\bar{G}^{-}_{0r}}. \tag{24}$$

This result is remarkable because it implies that $1/(1-t_q)$ diverges like q^{-2} for $q \sim 0$ and $\delta \sim 0$, reflecting the well-known undamped two-particle mode for diffusion [1–3].

4.2. Spinor Green's function

For the spinor Hamiltonian H_m of Eq. (3) we introduce the coordinate r and the Pauli matrix index $a = 1, 2$ and adopt the same procedure as for the scalar case. With the correlation $\langle V_{r,a}V_{r',a'}\rangle = g_{aa'}\delta_{r,r'}$ and with $\bar{G}^{+} = G_0(z)$, $\bar{G}^{-} = G_0(z)^{*}$ for $z = \mu - i\delta - i\eta$, where μ is the renormalized Fermi energy (i.e., the bare Fermi energy which is shifted by the real part of the self-energy Σ^{+}) and η is the scattering rate (i.e., the imaginary part of the self-energy). Now we use the Fourier representation of H_m and get with $h^2 = h_1^2 + h_2^2$ for Green's function

$$G_{0,k}(z) = \frac{-1}{z^2 - m^2 - h^2}(z\sigma_0 + h_1\sigma_1 + h_2\sigma_2 + m\sigma_3), \tag{25}$$

and

$$t_{q;ab,cd} = g_{cd}\int_k G_{0;k,ac}G^{*}_{0;q+k,bd},$$
$$\tau_{q;ab,cd} = g_{cb}\int_k G_{0;k,ac}G^{*}_{0;q+k,db}. \tag{26}$$

For random scalar potential $v\sigma_0$ (random gap $v\sigma_3$) the prefactors read $g_{11} = g_{22} = g_{12} = g_{21} \equiv g$ ($g_{11} = g_{22} = -g_{12} = -g_{21} \equiv g$), and for independent random diagonal elements $g_{11} = g_{22} \equiv g$, $g_{12} = g_{21} = 0$. Then we get from Eq. (26) for $q = 0$ the matrices

$$t_0 = \begin{pmatrix} \alpha_1 & 0 & 0 & \beta \\ 0 & s\alpha_2 & 0 & 0 \\ 0 & 0 & s\alpha_3 & 0 \\ \beta & 0 & 0 & \alpha_4 \end{pmatrix}, \quad \tau_0 = \begin{pmatrix} \alpha_1 & 0 & 0 & 0 \\ 0 & s\alpha_2 & \beta & 0 \\ 0 & \beta & s\alpha_3 & 0 \\ 0 & 0 & 0 & \alpha_4 \end{pmatrix}, \tag{27}$$

where $s = -1$ for a random gap, $s = 1$ for random scalar potential, $s = 0$ for independent random diagonal elements. For Dirac fermions we have $h_j = k_j$ and the matrix elements are the following expressions:

$$\alpha_1 = gI(z+m)(z^{*}+m), \quad \alpha_2 = gI(z+m)(z^{*}-m),$$
$$\alpha_3 = gI(z-m)(z^{*}+m), \quad \alpha_4 = gI(z-m)(z^{*}-m)$$

with

$$I = \int_k \frac{1}{|z^2 - m^2 - k^2|^2}, \quad \beta = g\int_k \frac{k^2}{|z^2 - m^2 - k^2|^2}. \tag{28}$$

Using the SCBA we obtain the integral (cf. Appendix A)

$$\int_k \frac{|z|^2 + m^2 + k^2}{|z^2 - m^2 - k^2|^2} = \frac{1}{g} - \frac{\delta}{g\eta}, \tag{29}$$

which implies $\beta \sim 1 - gI(|z|^2 + m^2)$ for $\delta \sim 0$. We consider two special cases now, the behavior at the Dirac node and the gapless case:

(I) *At the Dirac node* $\mu = 0$: For the Hamiltonian H_m of Eq. (3) we get the parameter $\beta \sim 1 - g(\eta^2 + m^2)I$, and the eigenvalues of $\mathbf{1} - t_0$ now read

$$\eta^{\pm}_{L} = 1 - gI(\eta^2 + m^2) \mp [1 - gI(\eta^2 + m^2)] = \begin{cases} 0 \\ 2 - 2gI(\eta^2 + m^2), \end{cases} \tag{30}$$

and the eigenvalues of $\mathbf{1} - \tau_0$ for $s = \pm 1$ read

$$\eta^{\pm}_{M} = 1 - s(\eta^2 - m^2)gI \pm \sqrt{[1 - gI(\eta - m)^2][1 - gI(\eta + m)^2]}. \tag{31}$$

Thus, the ladder contribution with η^{+}_{L} is always undamped, in contrast to η^{-}_{L} and the maximally crossed contributions $\eta^{\pm}_{M}$, which are all damped.

(II) *Gapless spectrum* $m = 0$: For the Hamiltonian H_0 we have $\beta \sim 1 - g|z|^2 I$, and the eigenvalues read

$$\eta^{\pm}_{L} = 1 - g|z|^2 I \mp (1 - g|z|^2 I) = \begin{cases} 0 \\ 2 - 2g|z|^2 I, \end{cases} \tag{32}$$

$$\eta^{\pm}_{M} = 1 - sg|z|^2 I \pm (1 - g|z|^2 I) = \begin{cases} (1-s)g|z|^2 I \\ 2 - (1+s)g|z|^2 I, \end{cases} \tag{33}$$

such that there is a undamped mode $\eta^{+}_{L} = 0$ for any s, like for the Dirac node, and an additional undamped mode from the maximally crossed contribution $\eta^{-}_{M} = 0$ for $s = 1$. These results are summarized in Table 1.

Table 1
Vanishing damping terms $\eta_{L,M}^{\pm}$ in the propagators $(\mathbf{1}-t_0)^{-1}$ and $(\mathbf{1}-\tau_0)^{-1}$ (cf. Eqs. (27), (30)–(33)).

Parameters	Independent random diagonal elements	Random scalar potential	Random gap
	$s=0$	$s=1$	$s=-1$
$\mu=0$	$\eta_L^+=0$	$\eta_L^+=0$	$\eta_L^+=0$
$m=0$	$\eta_L^+=0$	$\eta_L^+=0$, $\eta_M^-=0$	$\eta_L^+=0$

4.3. Diffusion propagator

The findings of the previous section can be used to evaluate the correlation function as

$$\langle G_{rr',ab}\, G^*_{rr',cd}\rangle \approx \frac{1}{g_{bd}}(\mathbf{1}-t)^{-1}_{rr';ac,bd} + \frac{1}{g_{bd}}(\mathbf{1}-\tau)^{-1}_{rr';ad,bc} - \frac{1}{g_{bd}}(t^2{}_{rr';ac,bd} + t_{rr';ac,bd} + 2\delta_{rr'}\,\delta_{ac}\,\delta_{bd}\,). \tag{34}$$

In general, the propagators read

$$(\mathbf{1}-t_q\,)^{-1} \sim (\delta+\eta_L+D_t\,q^2)^{-1}, \quad (\mathbf{1}-\tau_q\,)^{-1} \sim (\delta+\eta_M+D_\tau\,q^2)^{-1} \tag{35}$$

with the damping terms η_L and η_M. For the long-range behavior with $|r-r'|\sim\infty$ it is sufficient to consider the two-particle propagators $(\mathbf{1}-t_q\,)^{-1}$ and $(\mathbf{1}-\tau_q\,)^{-1}$ for $q\sim 0$ in Eq. (34). Then we can focus on the undamped (diffusion) modes as the most important contributions to get for $q\sim 0$

$$K_q \sim \frac{\eta}{\delta+D_{t,\tau}\,q^2} \to \frac{\eta}{-i\omega+D_{t,\tau}\,q^2}, \tag{36}$$

where the second expression is obtained by the analytic continuation $\delta\to -i\omega$. The diffusion coefficients $D_{t,\tau}$ are obtained from the q expansion of the eigenvalues of (26) as

$$D_t = \frac{g\eta}{2}\sum_r r_\mu^2[G_{0;r0,11}G^*_{\tilde{0};0r,11} + G_{0;r0,12}G^*_{\tilde{0};0r,12}] + o(g^2),$$

and additionally for $s=1$

$$D_\tau = \frac{g\eta}{2}\sum_r r_\mu^2[G_{0;r0,11}G^*_{\tilde{0};0r,22} + G_{0;r0,12}G^*_{\tilde{0};0r,12}] + o(g^2).$$

Both coefficients agree, at least up to terms of $o(g^2)$, and give us

$$D_t = D_\tau = \frac{g}{4\pi\eta}\left(1+\frac{1+\zeta^2}{\zeta}\arctan\,\zeta\right) + o(g^2) \quad (\zeta=\mu/\eta). \tag{37}$$

5. Corrections to the Boltzmann–Drude conductivity

Next, the results of the WLA will be used to evaluate the quantum corrections to the Boltzmann–Drude conductivity. For the present case we prefer to use the density–density Kubo formula [18–21]:

$$\sigma_{\mu\mu} = -\frac{e^2}{2h}\omega^2\sum_r r_\mu^2\,\mathrm{Tr}_2\langle G_{r0}\,G^\dagger_{0r}\rangle \tag{38}$$

rather than the current–current Kubo formula [15]. This expression is closely related to diffusion and the Einstein relation [9]. The classical approximation assumes a weak correlation between the two Green's functions G, $G^\dagger$ such that we can factorize the expectation value as $\langle G_{r0}\,G^\dagger_{0r}\rangle \approx \langle G_{r0}\rangle\langle G^\dagger_{0r}\rangle$ and obtain the Boltzmann–Drude conductivity as

$$\bar\sigma = -\frac{e^2}{2h}\omega^2\sum_r r_\mu^2\,\mathrm{Tr}_2\langle G_{r0}\rangle\langle G^\dagger_{0r}\rangle. \tag{39}$$

Furthermore, the average one-particles Green's functions are evaluated within the SCBA as $\langle G_{r0}\rangle\approx\bar G_{r0}$. For the gapless case $m=0$ and for the parameters $\chi=2\mu/\omega$, $\zeta=\mu/\eta$ we can write

$$\sum_r r_\mu^2\,\mathrm{Tr}_2\langle G_{r0}\rangle\langle G^\dagger_{0r}\rangle \approx \sum_r r_\mu^2\,\mathrm{Tr}_2\bar G_{r0}\,\bar G^\dagger_{0r} \approx \begin{cases} -\frac{1}{\pi\omega^2}\left[1+\frac{1}{4\chi}(1-\chi^2)\log\left(\frac{(1+\chi)^2}{(1-\chi)^2}\right)\right] & \text{for } \omega\gg\eta \\ \frac{1}{4\pi\eta^2}\left[1+\frac{1}{\zeta}(1+\zeta^2)\arctan\,\zeta\right] & \text{for } \omega\ll\eta. \end{cases} \tag{40}$$

In particular, for $\omega\gg\eta$ the Boltzmann–Drude conductivity reads

$$\bar\sigma = \frac{e^2}{2\pi h}\left[1+\frac{1}{4\chi}(1-\chi^2)\log\left(\frac{(1+\chi)^2}{(1-\chi)^2}\right)\right]. \tag{41}$$

This expression is obviously not the Boltzmann–Drude conductivity of a conventional metal with one-band Hamiltonian. At the Dirac node $\mu=0$ it has a frequency independent conductivity $\bar\sigma=e^2/h\pi$ and decreases monotonically from $e^2/h\pi$ to zero as we move the Fermi energy μ away from the Dirac node. This indicates a cross-over from the optical conductivity of the two-band model at the Dirac node to the Boltzmann–Drude behavior of a conventional metal, where the optical conductivity is much lower than in the two-band case. Here it should be noticed that there are additional corrections for $\omega\gg\eta$, which increase the optical conductivity to $\pi e^2/8$. These are not taken into account here, since they disappear in the DC limit [21]. For $\omega\ll\eta$, on the other hand, the Boltzmann approximation is invalid, which is reflected by a negative Boltzmann–Drude conductivity that vanishes like $\bar\sigma\propto\omega^2$. For this regime we must consider the corrections $\delta\sigma$ which can be evaluated from Eq. (34) as

$$\lim_{\omega\to 0}\omega^2\sum_r (r_\mu-r'_\mu)^2\langle G_{rr',ab}\,G^*_{rr',ab}\rangle \approx \frac{1}{g}\lim_{\omega\to 0}\omega^2\sum_r (r_\mu-r'_\mu)^2[(\mathbf{1}-t)^{-1}_{rr';aa,bb} + (\mathbf{1}-\tau)^{-1}_{rr';ab,ba}]. \tag{42}$$

With the help of the propagator in Eq. (36) and the diffusion coefficient (37) the conductivity corrections then read

$$\delta\sigma = \frac{e^2}{h}\omega^2\frac{\partial^2}{\partial q_l^2}\frac{\eta/g}{-i\omega+Dq^2}\bigg|_{q=0} = \frac{e^2}{hg}2\eta D = \frac{e^2}{2\pi h}\left(1+\frac{1+\zeta^2}{\zeta}\arctan\,\zeta\right) + o(g^2) \sim \frac{e^2}{\pi h}(1+\zeta^2/3). \tag{43}$$

There is an additional factor 2 for $s=1$ due to the extra undamped mode from $\eta_M^-=0$ in that case. This result, which is depicted in Fig. 2, agrees with previous calculations based on the WSA [9] as well as with the experimentally measured V-shape conductivity with respect to μ^2 in graphene [22,23].

6. Discussion

Our main result is that the ladder and the maximally crossed contributions are quite different for the spinor Hamiltonians, in contrast to their agreement for the scalar Hamiltonian of Section

4.1. This situation is reminiscent of the Bose–Fermi functional representation of the average two-particle Green's function in the case of Dirac fermions with a random gap, where it was observed that the bosonic and the fermionic propagators are distinct [8]. Similar to the expressions in Eq. (27), the inverse bosonic two-particle propagator of the WSA is also a 4×4 matrix for $a, \ldots, d = 1, 2$

$$\delta_{ac}\,\delta_{bd} - g\int_k G_{0;k,ac}(z)G_{0;k-q,bd}(z),$$

while its fermionic counterpart reads

$$\delta_{ac}\,\delta_{bd} - g\int_k G_{0;k,ac}(z)G_{0;-k-q,db}(z).$$

A straightforward calculation shows that only the fermionic propagator has a undamped mode, very similar to $\mathbf{1} - t_q$ with $s = -1$ of the WLA. Therefore, the comparison of the WSA with the WLA sheds some light on the role of Bose–Fermi (or super-) symmetry breaking, which can be associated with the difference between ladder diagrams and maximally crossed diagrams in the WLA. In particular, the undamped mode of the WLA agrees with the undamped fermion mode of the WSA, where the latter is caused by a spontaneous breaking of a non-Abelian chiral symmetry [8–10].

It remains to be discussed whether or not the structure of the diffusion poles is robust with respect to approximations. In the one-band projection of the one-particle Green's function the pole of the second band has been ignored [5–7], since it is energetically too far away from the Fermi surface. For $\mu > 0$ and $m=0$ we have

$$G_{0;k,ab} = U^*_{1a}\frac{1}{\epsilon(k)-z}U_{1b} + U^*_{2a}\frac{1}{-\epsilon(k)-z}U_{2b} \to U^*_{1a}\frac{1}{\epsilon(k)-z}U_{1b}$$
$$\text{with } U = \frac{1}{\sqrt{2}}\begin{pmatrix}\kappa^* & 1\\ -\kappa^* & 1\end{pmatrix} \tag{44}$$

and $\kappa = (k_1 - ik_2)/k \equiv e^{i\Phi(k)}$, which provides a spinor Green's function with a single pole

$$G_0 \approx \frac{1}{\epsilon_k - \mu + i\delta + i\eta}\frac{1}{2}(\sigma_0 - \sigma_1 k_1/k - \sigma_2 k_2/k). \tag{45}$$

For the projected Green's function the matrices (27) then read

$$t_0 = \frac{gI}{4}\begin{pmatrix}1&0&0&1\\0&s&0&0\\0&0&s&0\\1&0&0&1\end{pmatrix},\quad \tau_0 = \frac{gI}{4}\begin{pmatrix}1&0&0&0\\0&s&1&0\\0&1&s&0\\0&0&0&1\end{pmatrix},\quad I = \int_k \frac{1}{|k^2 - z|^2}, \tag{46}$$

where we get $gI = 2 - 2\delta/\eta$ from the SCBA. Thus the damping terms of the ladder diagram (i.e., the eigenvalues of $\mathbf{1} - t_0$) are $0, 1, 1 - s/2, 1 - s/2$ and the damping terms of the maximally crossed diagrams (i.e. the eigenvalues of $\mathbf{1} - \tau_0$) are $1 - (s+1)/2, 1 - (s-1)/2, 1/2, 1/2$. Like in the case of the two-band Green's function of Section 4.2 there is one undamped mode for $\mathbf{1} - t_0$ for any value of s and one undamped mode for $\mathbf{1} - \tau_0$ if $s=1$. This indicates that the result of the one-band projection preserves the structure of two-band result of Table 1 in terms of the number of undamped modes. The agreement of the results from the one-band projected Green's function and the two-band Green's function reflects the fact that the type of diffusive modes is not sensitive to the scattering to the second band.

6.1. Inter-node scattering

Finally, we briefly discuss the effect of inter-node scattering for the Hamiltonian H_0. For this purpose we introduce the extended Hamiltonian

$$\bar{H}_0 = \begin{pmatrix}H_0 & \nu\sigma_0\\ \nu\sigma_0 & H_{\bar{0}}^*\end{pmatrix}, \tag{47}$$

which describes inter-node scattering by the random scattering terms $\nu\sigma_0$.

Now we could evaluate the inverse two-particle Green's functions within the WLA and study the vanishing eigenvalues, which would be associated with diffusive behavior. Alternatively, we can also start from the symmetry argument and analyze the underlying chiral symmetry whose spontaneous breaking would create an undamped mode, analogously to the treatment of random scattering terms in Ref. [9]. Following this concept, we first realize that the Hamiltonian $\bar{H}_0$ changes its sign under the transformation in Eq. (4)

$$\bar{H}_0 \to S\bar{H}_0 S = -\bar{H}_0,\quad S = \begin{pmatrix}\sigma_3 & 0\\ 0 & -\sigma_3\end{pmatrix}. \tag{48}$$

According to the general procedure of Ref. [9], this leads for the Hamiltonian $\hat{\bar{H}}_0 = \mathrm{diag}(\bar{H}_0, \bar{H}_0)$ to the non-Abelian chiral symmetry

$$e^{\hat{S}}\hat{\bar{H}}_0 e^{\hat{S}} = \hat{\bar{H}}_0,\quad \hat{S} = \begin{pmatrix}0 & \varphi S\\ \varphi' S & 0\end{pmatrix} \tag{49}$$

for independent continuous parameters φ, φ', since $\hat{\bar{H}}_0$ and $\hat{S}$ anticommute. This symmetry is spontaneously broken due to the scattering rate η, causing the appearance of an undamped mode. Here it should be noticed though that the appearance of an undamped mode is only a necessary but not a sufficient condition for a diffusive behavior because the interaction of the nonlinear symmetry fields generated by φ, φ', could lead to Anderson localization [24,25].

7. Conclusions

The calculation of the ladder and maximally crossed contributions of the average two-particle Green's function has revealed a characteristic diffusion pole structure. Depending on the type of randomness, the ladder contributions always have one diffusion pole, provided the Fermi energy is at the Dirac node or away from the Dirac node but in the absence of a gap. Moreover, for a random scalar potential there is an additional diffusion pole from the maximally crossed contributions. All these results require the existence of a nonzero scattering rate, obtained as a solution of the self-consistent Born relation (SCBA).

The diffusion pole structure of the WLA is identical to that of the WSA, at least for the case of a random gap. This enabled us to identify the origin of the diffusion poles with undamped modes which are created by spontaneously broken symmetries. These are chiral symmetries, associated with the symmetry of the two bands. Such a symmetry exists also in the presence of inter-node scattering. Further work is necessary, though, to compare the relation between the WLA and the WSA for other types of disorder scattering.

The diffusion pole structure of the two-particle Green's function is preserved when we employ a one-band projection of the one-particle Green's function by removing one pole of the latter. Although this projection changes the form of the diffusion coefficient (cf. [5,6]), it may serve as a good approximation that reduces the computational effort significantly.

As already mentioned in the Introduction, the existence of a diffusion pole is a necessary condition but does not guarantee a metallic behavior. Higher order terms beyond the ladder and maximally crossed contribution can destroy diffusion and eventually lead to Anderson localization. This was studied recently in

terms of a strong scattering expansion [24,25], which revealed an exponential decay when the scattering rate η is larger than the band width E_b.

Acknowledgment

We are grateful to E. Hankiewicz, D. Schmeltzer and G. Tkachov for inspiring discussions.

Appendix A. Self-consistent Born approximation

The self-consistent equations (10) and (11) read in the case of Dirac fermions

$$z - \mu + i\delta = -\, g \int_k \frac{z}{z^2 - m^2 - k^2}$$

Subtracting its complex conjugate yields

$$z - z^* + 2i\delta = g(z - z^*) \int_k \frac{|z|^2 + m^2 + k^2}{|z^2 - m^2 - k^2|^2},$$

which in the limit $\delta \to 0$ becomes

$$\frac{1}{g} = \int_k \frac{|z|^2 + m^2 + k^2}{|z^2 - m^2 - k^2|^2}.$$

References

[1] L.P. Gorkov, A.I. Larkin, D.E. Khmelnitskii, Pisma v ZhETF 30 (1979) 248; L.P. Gorkov, A.I. Larkin, D.E. Khmelnitskii, JETP Lett. 30 (1979) 228.
[2] S. Hikami, A.I. Larkin, Y. Nagaoka, Prog. Theor. Phys. 63 (1980).
[3] B.L. Altshuler, A.G. Aronov, P.A. Lee, Phys. Rev. Lett. 44 (1980) 1288; B.L. Altshuler, D. Khmel'nitzkii, A.I. Larkin, P.A. Lee, Phys. Rev. B 22 (1980) 5142.
[4] T. Ando, Y. Zheng, H. Suzuura, J. Phys. Soc. Japan 71 (2002) 1318; H. Suzuura, T. Ando, Phys. Rev. Lett. 89 (2002) 266603; E. McCann, et al., Phys. Rev. Lett. 97 (2006) 146805.
[5] D.V. Khveshchenko, Phys. Rev. Lett. 97 (2006) 036802.
[6] G. Tkachov, E.M. Hankiewicz, Phys. Rev. B 84 (2011) 035444.
[7] D. Schmeltzer, A. Saxena, Phys. Rev. B 88 (2013) 035140.
[8] K. Ziegler, Phys. Rev. B 55 (1997) 10661.
[9] K. Ziegler, Eur. Phys. J. B 86 (2013) 391.
[10] K. Ziegler, Phys. Rev. Lett. 80 (1998) 3113.
[11] L. Schäfer, F. Wegner, Z. Phys. B 38 (1980) 113.
[12] K. Efetov, Supersymmetry in Disorder and Chaos, Cambridge University Press, Cambridge, 1997.
[13] S. Raghu, S.B. Chung, X.-L. Qi, S.-C. Zhang, Phys. Rev. Lett. 104 (2010) 116401; X.-L. Qi, S.-C. Zhang, Rev. Mod. Phys. 83 (2011) 1057.
[14] J.S. Langer, T. Neal, Phys. Rev. Lett. 16 (1966) 984.
[15] The inequivalence of the current-current and density-density formula in the DC limit is discussed in A. Sinner, K. Ziegler, Phys. Rev. B 89 (2014) 024201.
[16] S.V. Morozov, K.S. Novoselov, M.I. Katsnelson, F. Schedin, L.A. Ponomarenko, D. Jiang, A.K. Geim, Phys. Rev. Lett. 97 (2006) 016801.
[17] F.V. Tikhonenko, D.W. Horsell, R.V. Gorbachev, A.K. Savchenko, Phys. Rev. Lett. 100 (2008) 056802.
[18] D.J. Thouless, Phys. Rep. 13 (1974) 93.
[19] F.J. Wegner, Phys. Rev. B 19 (1979) 783.
[20] A.J. McKane, M. Stone, Ann. Phys. 131 (1981) 36.
[21] K. Ziegler, Phys. Rev. B 78 (2008) 125401.
[22] K.S. Novoselov, A.K. Geim, S.V. Morozov, D. Jiang, M.I. Katsnelson, I. V. Grigorieva, S.V. Dubonos, A.A. Firsov, Nature 438 (2005) 197.
[23] Y. Zhang, Y.-W. Tan, H.L. Stormer, P. Kim, Nature 438 (2005) 201.
[24] A. Hill, K. Ziegler, Physica E 56 (2013) 172.
[25] K. Ziegler, arXiv:1404.2146.